

Conservative self-organized extremal model for wealth distribution

Abhijit Chakraborty¹, G. Mukherjee^{1,2} and S. S. Manna¹

¹*Satyendra Nath Bose National Centre for Basic Sciences, Block-JD, Sector-III, Salt Lake, Kolkata-700098, India*

²*Bidhan Chandra College, Asansol 713304, Dt. Burdwan, West Bengal, India*

We present a detailed numerical analysis of the modified version of a conservative self-organized extremal model introduced by Pianegonda et. al. for the distribution of wealth of the people in a society. Here the trading process has been modified by the stochastic bipartite trading rule. More specifically in a trade one of the agents is necessarily the one with the globally minimal value of wealth, the other one being selected randomly from the neighbors of the first agent. The pair of agents then randomly re-shuffle their entire amount of wealth without saving. This model has most of the characteristics similar to the self-organized critical Bak-Sneppen model of evolutionary dynamics. Numerical estimates of a number of critical exponents indicate this model is likely to belong to a new universality class different from the well known models in the literature. In addition the persistence time, which is the time interval between two successive updates of wealth of an agent has been observed to have a non-trivial power law distribution. An opposite version of the model has also been studied where the agent with maximal wealth is selected instead of the one with minimal wealth, which however, exhibits similar behavior as the Minimal Wealth model.

PACS numbers: 89.65.Gh, 87.23.Ge, 05.65.+b, 64.60.Ht.

1. INTRODUCTION

Study of the probability distribution of wealth of the people in a society goes back to 1897 when Pareto observed empirically that the distribution is characterized by a power law tail. Probability that an individual member has wealth more than w is given by $P(w) \sim w^{1-\alpha}$ with $\alpha = 5/2$ [1]. This type of distribution is known as the Pareto distribution [2]. This observation reflects the inherent inequality in the economic structure of the society. A large number of individuals are economically poor. In comparison the number of wealthier people is less and their number gradually decreases as their wealth increases. The cut-off of the distribution corresponds to with few very rich individuals. Consequently a sizable fraction of the society's net wealth is in fact possessed by a class of top rich people consisting only a few percent of society's entire population. Since measuring wealth is difficult, in recent years distributions of income and tax return amounts have been studied in different countries. For example tax return amount distribution in US and Japan shows a log-normal distribution in the middle range followed by a power law for high income people [3], UK data of income shows an exponential decay which is followed by a power law in the high income range [4] and income data in Brazil for 2004 shows an almost Gaussian law for the low and middle income groups where as high salary groups are described approximately by power law [5].

A good amount of research effort has been devoted in recent times to study the wealth distribution using the ideas of Statistical Physics. In this description an individual member is called an agent. The microstate specified by the precise description of wealth of every agent changes after each transaction. Their wealth change due to interaction among themselves. This interaction is the

mutual bipartite trade among different pairs of agents. Thus the wealth distribution evolves due to such repeated interactions and finally assumes a time independent form.

In a simple model the total wealth of the entire society has been considered as strictly conserved. In a transaction the net amount of wealth of the pair of agents is randomly re-shuffled between them and therefore the pairwise interactions also maintain conservation of wealth [6, 7]. Starting from an arbitrary initial distribution of wealth with a fixed average value the system attains a steady state. The steady state wealth distribution has been found to have an exponentially decaying tail. Such distribution was also observed in [8]. In a subsequent modification of the model saving propensity factor λ has been introduced where each trader invests only $1 - \lambda$ fraction of his wealth to the bipartite trade [9]. With a fixed value of λ the steady state wealth distribution becomes very similar to the Gamma distribution [10, 11]. This model was further extended by assigning quenched saving propensities λ_i specific to each individual agent [12–14]. Here one gets a power law tail with $\alpha \approx 2.0$ only when wealth distributions are averaged over different $\{\lambda_i\}$ sets [12, 15]. All these results exhibit economic inequality in the society. A review of all these models has been published in [16].

Apart from these a different idea of extremal dynamics for the evolution of wealth distribution has been studied by Pianegonda et. al. on an one dimensional ($1d$) lattice [17, 18]. It is assumed that always the poorest agent of the society initiates a trade since he feels the strongest urge to raise its economic status. The trade is implemented by locating the poorest agent and refreshing his wealth randomly. To ensure that the model remains strictly conserved, the amount of wealth gained by the minimal site has been taken out equally from its two neighbors. Consequently this model allows an agent to

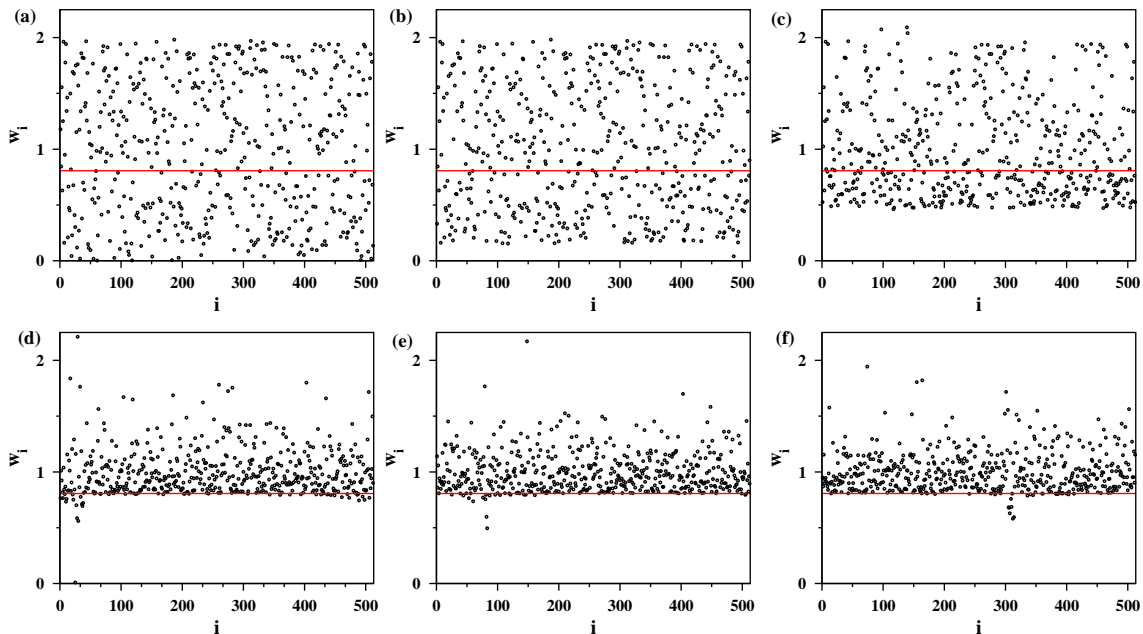


FIG. 1: (Color online) Time evolution of the wealth w_i at different sites of an $1d$ lattice of size $N = 512$. The series of snapshots are taken at times $t =$ (a) 0, (b) 500, (c) 1000, (d) 500000, (e) 5000000 and (f) 15000000. The position of the poverty line at $w_c^{half}(512) = 0.8070$ is shown by the red line. With time the wealth values gradually move up beyond the poverty line and stays there in the stationary state during further evolution.

possess a negative wealth. In the stationary state of large systems $P(w)$ jumps from zero to a maximal value at a critical value of w_c and then it decays as w increases as the Boltzmann-Gibbs exponential function.

The Pianegonda model is very similar to the non-conservative self-organized extremal model for the ecological evolution of interacting species introduced by Bak and Sneppen (BS) [19]. The phenomenon of Self-organized Criticality (SOC) is the spontaneous emergence of fluctuations of all length and time scales in a slowly driven system. This concept was first introduced to describe the formation of a sandpile of a fixed shape [20]. Later the idea of SOC has been applied to a large number of different physical systems [21]. In a stochastic version of the sandpile model grains are distributed to randomly selected neighboring sites [22]. In the SOC models fluctuations are described in terms of avalanches of activities and their size distributions assume power law decaying functions for large system sizes. In BS model an entire species is represented by a single fitness variable. A set of species is represented by the nodes of a graph. Using the spirit of Darwinian principle in each mutation the fitness of the node with globally minimal value is searched and is refreshed by a new random value. Effect of this propagates to few neighboring nodes which are also refreshed. The system eventually reaches a stationary state when the fitness distribution assumes a time independent step like form.

An absorbing state phase transition in presence of a

conserved continuous local field has been studied recently [23]. In this model a pair of sites is said to be active if at least one of them has energy more than a pre-assigned threshold. An active pair re-shuffles its net energy between them keeping the energy strictly conserved. Beyond a critical value of the threshold the number of active pairs fluctuates with time in the stationary state and the time averaged density of active pairs has been considered as the order parameter for the problem. As the threshold value is tuned a continuous phase transition is observed from an absorbing phase to an active phase [23]. It was claimed that the critical exponents of this model are different from the Directed Percolation model.

In a related model defined for the wealth distribution at least one of the agents in a bipartite trading is selected from a subset of agents [24]. This subset is formed by agents who have wealth less than certain upper cutoff, the other agent being selected randomly from the neighbors of the first agent. In a transaction the net wealth of the pair of agents is randomly re-shuffled between them. The order parameter has been defined as the fraction of agents having wealth below a certain threshold value and it is claimed that the system undergoes a continuous phase transition at a critical value of the threshold wealth. A number of critical exponents have been measured to characterize the transition and some of them are found to be close to corresponding exponents in the Manna model of Self-organized Critically [22].

In this paper we present a detailed numerical analysis

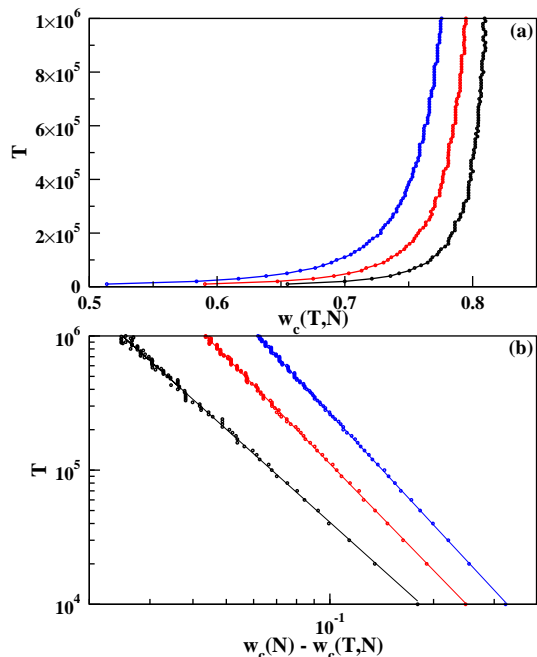


FIG. 2: (Color online) The system is relaxing from initial state to the stationary state for $N = 2^{10}$ (black), 2^{11} (red) and 2^{12} (blue). (a) The relaxation time T has been plotted with the corresponding position of the poverty line $w_c(T, N)$. (b) The same data has been plotted with deviation $w_c(N) - w_c(T, N)$ on a log – log scale. The slopes are -2.30 , -2.64 and -2.76 respectively, which on extrapolation give the value of the dynamical exponent $z \approx 2.84$.

of the modified Pianegonda et. al. model whose trading rule has been replaced by the stochastic re-shuffling of the net wealth of a pair of agents. We consider this model as one of the few examples of non-dissipative SOC systems where the entire wealth of the society is strictly conserved, for example the fixed energy sandpile [25]. Estimation of a number of critical exponents of the modified Pianegonda et. al. model suggests that this model does not belong to the universality class of either BS model or Manna model. We believe that it belongs to a new universality class perhaps because of strict conservation of wealth is maintained in its dynamical rules. The model studied by us in this paper and that in [24] are essentially same but studied from two different approaches. An approach which is very typical of a SOC system has been followed by us where the critical poverty line spontaneously evolves without any fine tuning. In contrast in [24] the position of the poverty line is tuned by hand to arrive at the critical state.

In section 2 we describe the Minimal Wealth model where the trader with minimal wealth initiates the trade. In subsection 2.1 we discuss the relaxation dynamics of the system on its way to the stationary state. In subsection 2.2 the correlation that evolves in the system in

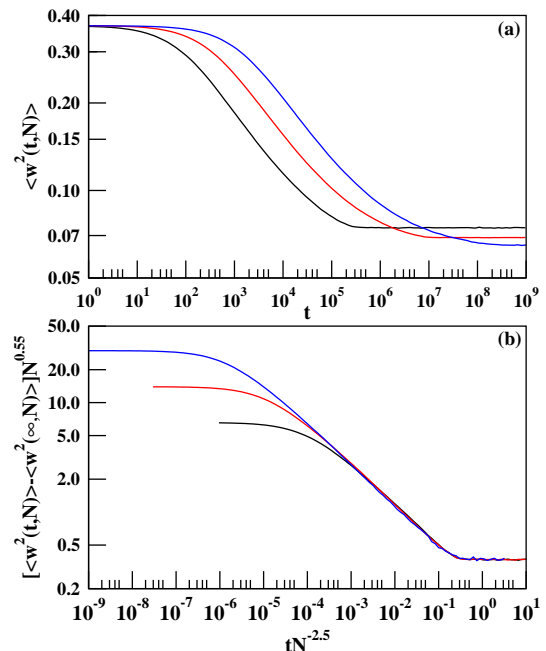


FIG. 3: (Color online) Estimating the relaxation times. (a) The average wealth square $\langle w^2(t, N) \rangle$ per agent has been plotted with time t for $N = 2^8$ (black), 2^{10} (red) and 2^{12} (blue) and after a long time they approach the stationary state value $\langle w^2(\infty, N) \rangle$. (b) The scaled deviation $[\langle w^2(t, N) \rangle - \langle w^2(\infty, N) \rangle] N^{0.55}$ has been plotted with the scaled variable $tN^{-2.5}$. The relaxation exponent $z = 2.70$.

the stationary state is studied. Wealth distribution in the stationary state is described in subsection 2.3. The statistics of the avalanche life-time distributions has been studied in section 2.4. This section ends with the study of persistence time distribution of individual agent's wealth in subsection 2.5. In section 3 we have described the Maximal Wealth model, which is opposite to the Minimal Wealth model, where the trader with maximal wealth initiates the trade. Finally we conclude in section 4.

2. THE MINIMAL WEALTH MODEL

In this paper we have considered a model with a conservative extremal dynamics for studying the evolution of wealth distribution in a society. In a bipartite transaction one agent is necessarily selected as the one with the globally minimal value of wealth w_{min} . The second agent is chosen randomly with uniform probability from neighbors of the first agent. This neighbor list has been defined in different ways for different graphs. We have studied this model on four different graphs, namely, (i) $1d$ regular lattice with periodic boundary condition (ii) two dimensional ($2d$) square lattice with periodic boundary condition (iii) the Barabási - Albert (BA) scale-free graph [26] and on an (iv) N -clique graph. On every graph

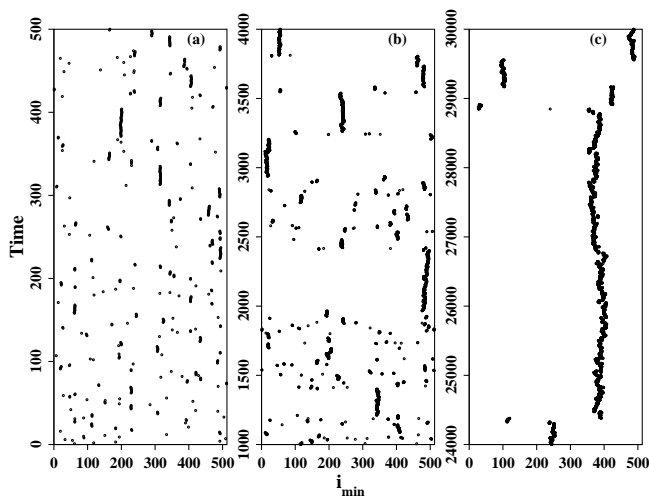


FIG. 4: An exhibition of the correlation that sets in the system. In a single run the lattice sites i_{min} with globally minimal wealth in successive time steps are marked for a system of size $N = 512$ in $1d$. The gradually increasing duration of correlation has been exhibited by time windows of increasing lengths: (a) 500, (b) 3000 and (c) 6000.

the nodes represent agents and the nearest neighbors of each node connected by direct links constitute the neighbor list of every agent. We report elaborately the results of our model on an $1d$ lattice and mention the key results of the same model studied on other graphs in tables.

The dynamics starts with N agents, each having an amount of wealth $w_i, \{i = 1, N\}$ drawn from a uniform distribution with the average $\langle w(N) \rangle = 1$ irrespective of the system size N . The discrete time t is the number of bipartite transactions. At an arbitrary time t first the site $i = i_{min}$ is searched out which has the minimal wealth w_{min} . The other agent j is selected randomly with uniform probability from the neighbors of i_{min} . Both agents invest their entire amount of wealth. Therefore the total invested amount by both the traders is: $\delta_{ij}(t) = w_i(t) + w_j(t)$. This amount is then randomly divided into two parts and received by them also randomly:

$$w_i(t+1) = \epsilon(t)\delta_{ij}(t) \quad w_j(t+1) = \bar{\epsilon}(t)\delta_{ij}(t). \quad (1)$$

where $\epsilon(t)$ is a freshly generated random fraction and $\bar{\epsilon} = 1 - \epsilon$. These transactions are repeated ad infinitum. After some relaxation time the system reaches a stationary state when the wealth distribution assumes a time independent form.

In $1d$ a linear chain of N sites with periodic boundary condition has been considered where the neighbor list of an arbitrary site i consists of the two nearest neighboring sites at $i \pm 1$. Therefore the second agent j is selected randomly with equal probability from this list. If w_{min} is very small then the probability that it will be replaced by an even smaller wealth after trade is also small. However

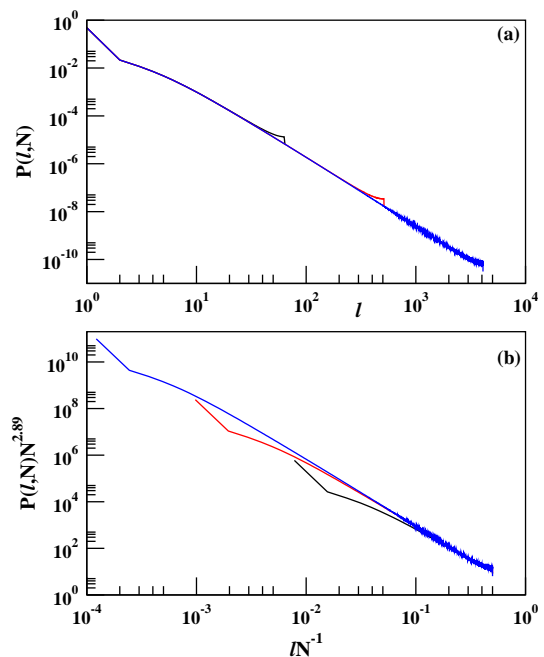


FIG. 5: (Color online) (a) The probability $P(\ell, N)$ that sites with minimal wealth at successive time steps are separated by a distance ℓ has been plotted with ℓ for the system sizes $N = 2^7$ (black), 2^{10} (red) and 2^{13} (blue). The slopes are -2.64, -2.81 and -2.89. (b) The finite-size scaling of $P(\ell, N)N^{\eta_\pi}$ vs. $lN^{-\zeta_\pi}$ with $\eta_\pi = 2.89$ and $\zeta_\pi = 1$ and therefore $\pi = \eta_\pi/\zeta_\pi = 2.89(5)$.

this probability gradually increases as w_{min} increases. As the sites with the minimal values of wealth are systematically replaced, very soon all nodes with small w values are replaced by larger values of w resulting a vacancy in the small w region. This is explained pictorially in Fig. 1. On an $1d$ lattice with $N = 512$ we plot the lattice positions i along the abscissa and the corresponding wealth w_i along the ordinate. As time increases a vacant region gradually forms for small values of w for all sites. If on the average the wealth of none of the agent is below a certain threshold value w , it is called the ‘poverty line’. In Fig. 1 the poverty line gradually moves up with time and finally settles at a critical value $w_c^{half}(512) = 0.8070$ at the stationary state. This behavior is the same for all system sizes N but with different values of $w_c(N)$. Unlike the model in [24] here the critical poverty line is spontaneously determined by the dynamical evolution of the system where no fine tuning is necessary which is the distinctive signature of self-organization and we will see in the following that the model exhibits critical behavior as well.

To find the agent with minimal wealth a brute-force search takes $\text{cpu} \sim N$. A much faster algorithm to search for the globally extremal (minimal or maximal) site was proposed by Grassberger [27, 28] which stores the data

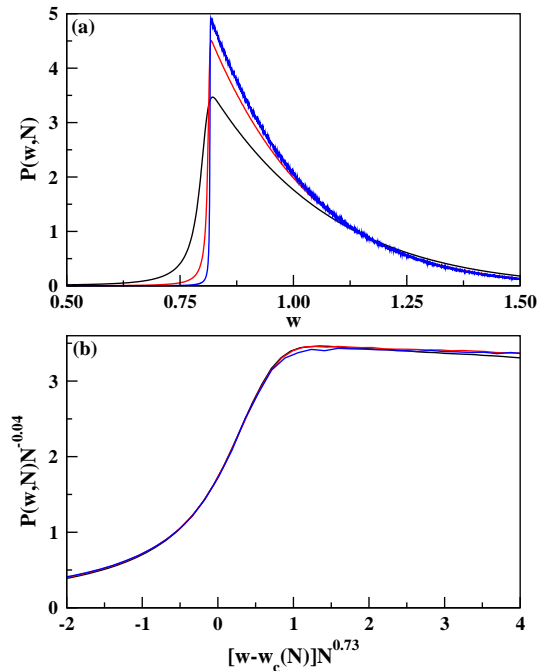


FIG. 6: (Color online) For Minimal Wealth model in $1d$. (a) The wealth distribution $P(w, N)$ in the stationary state for $N = 2^7$ (black), 2^{10} (red) and 2^{13} (blue). (b) A finite-size scaling using $P(w, N)N^{-0.04}$ vs. $[w - w_c(N)]N^{0.73}$ for system sizes $N = 2^{11}$ (black), 2^{12} (red) and 2^{13} (blue).

in a Hierarchical structure. This takes $\text{cpu} \sim \ln N$. We have used this method for $1d$, $2d$ and for N -clique graphs. For BA graphs we used the brute-force algorithm.

2.1 Relaxation to Stationary State

We first estimate the relaxation time required for the system to reach the stationary state. During this relaxation period the wealth distribution gradually changes starting from its initial uniform distribution to its time independent form in the stationary state. The relaxation time has been estimated as a function of deviation of the poverty line from its critical value in two ways.

For a given system size N we have simulated our model up to 10^6 time steps and calculated the wealth distribution $P(T, w, N)$ at 100 time instants T at the interval of 10^4 steps. These distributions are calculated for a sample size of $\sim 10^6$ independent runs. The value of the poverty line $w_c(T, N)$ at time T is determined by the value of w where $P(T, w, N)$ is the maximum. This estimation is done for all values of T . In Fig. 2(a) we plot on a $\ln - \ln$ scale T vs. $w_c(T, N)$ for $N = 2^{10}$, 2^{11} and 2^{12} . We see that in each case the relaxation time T diverges as $w_c(T, N)$ approaches its stationary state value $w_c(N)$. These data have been replotted in Fig. 2(b) using a log-log scale as T vs. $w_c(N) - w_c(T, N)$ where we

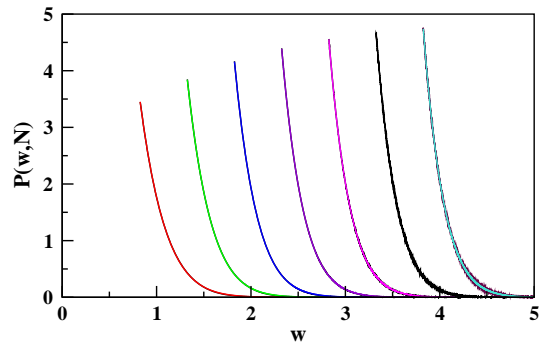


FIG. 7: (Color online) Gaussian fit of the wealth distribution $P(w, N)$ in the stationary state for seven different system sizes $N = 2^7$ to 2^{13} in $1d$. The sequence starts with the distribution for $N = 2^7$ at the extreme left and is shifted to the right by 0.2 when system size is multiplied by a factor of 2.

have used $w_c(N) = 0.8242$, 0.8375 and 0.8383 to obtain the best straight line plots. The slopes of these straight lines are 2.30, 2.64 and 2.76 respectively which are then extrapolated with $N^{-1.503}$ to obtain the exponent z as $T(N) \propto [w_c(N) - w_c(T, N)]^{-z}$ with $z \approx 2.84$.

In a second method we calculated $\langle w^2(t, N) \rangle$ with time t starting from its initial value when the distribution is uniform. After a long time this quantity saturates to its stationary value $\langle w^2(\infty, N) \rangle$. In Fig. 3(a) we show the plots of $\langle w^2(t, N) \rangle$ vs. t on a log-log scale. In Fig. 3(b) $[\langle w^2(t, N) \rangle - \langle w^2(\infty, N) \rangle]N^{0.55}$ has been plotted with the scaled value of time $tN^{-2.5}$ using $\langle w^2(\infty, N) \rangle = 0.057$, 0.0607 and 0.061 for $N = 2^8$, 2^{10} and 2^{12} respectively. A nice data collapse has been obtained with the following scaling form

$$[\langle w^2(t, N) \rangle - \langle w^2(\infty, N) \rangle]N^{0.55} \sim \mathcal{F}_z(tN^{-2.5}) \quad (2)$$

where the scaling function $\mathcal{F}_z(x)$ varies as $x^{-1/z}$ for small x . A direct measurement of the slope of the scaled plot gives an estimate of $1/z = 0.37$ which corresponds to $z = 2.70$. We conclude an average value of $z = 2.77(7)$.

2.2 Correlation in the Stationary State

Starting from an uncorrelated wealth distribution the system becomes more and more correlated as time passes. This is reflected in the fact that the probability of occurrence of the minimal sites close to each other in successive time steps gradually increases. At the early uncorrelated stage the position of the minimal site at the next time step is likely to be anywhere in the lattice. However as time increases, the poverty line moves up, consequently w_{min} increases and the probability that the minimal site at the next time step occurring at the same site or at the neighboring updated site also increases. This is shown in Fig. 4 using a $1d$ lattice of $N = 512$. For a single

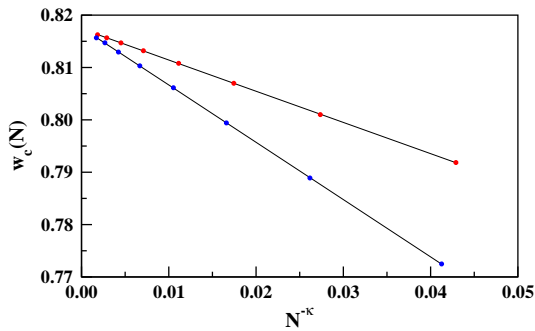


FIG. 8: (Color online) Estimation of the critical poverty line $w_c(\infty)$. The $w_c^{half}(N)$ are the upper plot (in red) and $w_c^{slope}(N)$ are the lower plot (in blue). When they are extrapolated with $N^{-\kappa}$ with $\kappa(half) = 0.649$ and $\kappa(slope) = 0.657$, $w_c(\infty)$ is obtained as 0.8174 and 0.8176 respectively. We conclude $w_c(\infty) = 0.8175(2)$.

run it is observed that the locations of w_{min} are quite random (Fig. 4(a)). However as time evolves these positions gradually become more correlated (Figs. 4(b) and 4(c)). In general one can consider the successive jumps of i_{min} positions constituting a Lévy flight random walk [29]. We see below that indeed their flight lengths follow a power law distribution.

The correlation in the stationary state is quantitatively measured by the probability distribution $P(\ell)$ of the distance of separation ℓ between successive minimal sites using periodic boundary condition. This distribution measured in the stationary state has been plotted in Fig. 5(a) for different system sizes $N = 2^7, 2^{10}$ and 2^{13} . The value of $P(\ell)$ for $\ell = 0$ and 1 are approximately 0.4575(1) and 0.4820(1) and then it decreases as a power law $P(\ell) \sim \ell^{-\pi}$ with increasing ℓ . A direct measurement of slope gives $\pi \approx 2.89$. Fig. 5(b) exhibits the finite-size scaling of the same data when the ℓ and $P(\ell, N)$ axes are scaled as:

$$P(\ell, N)N^{\eta\pi} \propto \mathcal{F}_\pi(\ell N^{-\zeta\pi}). \quad (3)$$

where $\mathcal{F}_\pi(x)$ is a universal scaling function with the scaling exponents $\eta_\pi = 2.89$ and $\zeta_\pi = 1$. From this scaling analysis we get $\pi = \eta_\pi/\zeta_\pi = 2.89(5)$.

There exists a spatial correlation too in this model. A two point correlation function has been measured in the stationary state. The average correlation between two sites situated at a distance of separation x has been defined as:

$$\mathcal{C}(x) = \langle w(0)w(x) \rangle - \langle w \rangle^2 \quad (4)$$

where $\langle w \rangle$ is always set equal to unity. We assume a power law decay for the correlation, i.e., $\mathcal{C}(x) \sim x^{-\chi}$ for $x \rightarrow \infty$. For 1d a plot of (not shown) $\mathcal{C}(x)$ vs. x on a log-log scale indicates a power law for large x values. However considerable variation of slopes exists for system

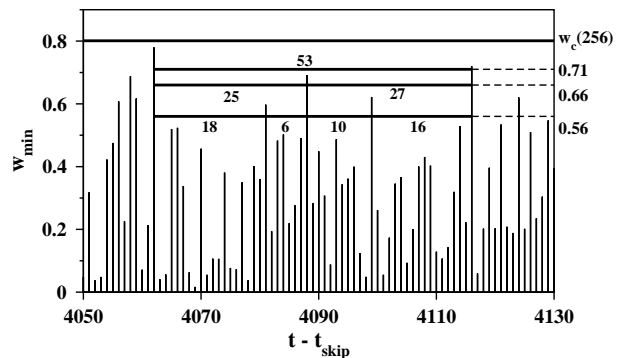


FIG. 9: A portion of the time series of minimal wealth values in successive time steps is shown for a 1d system with $N = 256$ and $w_c(256) = w_c^{half}(256) = 0.8010$ in the stationary state. It shows that depending on the value of w_o an avalanche can be broken into a hierarchy of avalanches. For this run the system has been relaxed for the initial $t_{skip} = 5 \times 10^8$ time steps.

sizes $N = 2^8, 2^{10}$ and 2^{12} . The slopes are: -1.17, -1.29, -1.34 respectively which extrapolates to a value of $\chi = 1.5(1)$ in the limit of $N \rightarrow \infty$. Our estimate for χ in 2d is 2.2(2).

2.3 Wealth Distribution in the Stationary State

Next we estimated the probability density distribution $P(w, N)$ of wealth in the stationary state of the system of size N . The distribution grows very rapidly near $w_c(N)$ for all values of N and then decays very fast. In Fig. 6(a) we show the plot of $P(w, N)$ vs. w for $N = 2^7, 2^{10}$ and 2^{13} . All of them have similar variations but with increasing system size the curves gradually become sharper. Therefore we tried a finite-size scaling analysis in Fig. 6(b) for the growing region and for $N = 2^{11}, 2^{12}$ and 2^{13} . A nice data collapse is observed when axes are scaled and $P(w, N)N^{-0.04}$ has been plotted with $[w - w_c(N)]N^{0.73}$.

The functional form of the decay of the probability distribution $P(w, N)$ has been studied right after the maximal jump at $w_c(N)$. This part fits very well with the Gaussian form:

$$P(w, N) = \frac{A(N)}{\sqrt{2\pi}\sigma(N)} \exp\left[-\frac{(w - \mu(N))^2}{2\sigma^2(N)}\right] \quad (5)$$

In Fig. 7 we showed $P(w, N)$ vs. w on a *lin-lin* scale for seven different system sizes: $N = 2^7, 2^8, \dots, 2^{13}$. In each case the fitting curve is indistinguishable from the data. We observe a systematic variation of $A(N)$, $\mu(N)$ and $\sigma(N)$ with system size N . For example $A(N) \approx 511.5 - 1828N^{-0.294}$, $\mu(N) \approx -1.10 + 62.5N^{-1.215}$ and $\sigma(N) \approx 0.64 + 0.429N^{-0.436}$.

The precise value of $w_c(\infty)$ is calculated by extrapolating $w_c(N)$ values which are calculated using the fol-

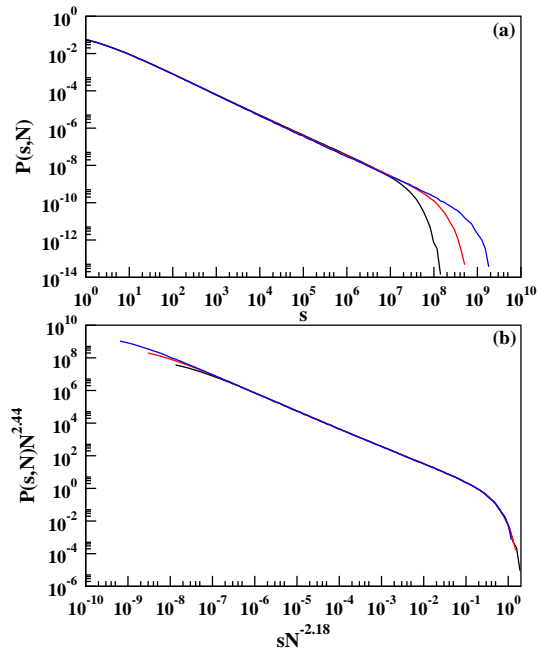


FIG. 10: (Color online) For 1d Minimal Wealth model. (a) The avalanche size distribution for $N = 2^{12}$ (black), 2^{13} (red) and 2^{14} (blue). (b) A finite-size scaling of the data in (a) with scaling exponents $\eta_\tau = 2.44$ and $\zeta_\tau = 2.18$ giving the avalanche size exponent $\tau = \eta_\tau/\zeta_\tau \approx 1.12(1)$.

lowing two methods. We have seen in Fig. 6(a) that the probability distribution of $P(w, N)$ becomes increasingly steeper with increasing N . For a certain size N we defined $w_c^{half}(N)$ as the value of w for which $P(w, N)$ is half of its maximum value. In a second method the $w_c(N)$ has been calculated in the following way. A pair of successive points on the $P(w, N)$ vs. w curve which has the largest slope is found out. A straight line joining these two points is then extrapolated to meet the w axis at $w_c^{slope}(N)$. The pair of values of $w_c^{half}(N)$ and $w_c^{slope}(N)$ for eight N values 2^7 to 2^{14} are then extrapolated with $N^{-\kappa}$. A least square fit of straight line has been done for trial values of κ starting from 0.20 to 1.20 at an interval of 0.001 and the errors have been calculated. The errors are minimal for $\kappa(half) = 0.649$ and $\kappa(slope) = 0.657$. Using these two values of the exponent κ we extrapolate $w_c(N)$ values with $N^{-\kappa}$ in Fig. 8 to meet the $w_c(N)$ axis at 0.8174 and 0.8176 respectively. We conclude a value for $w_c(\infty)$ for 1d model as 0.8175(2).

2.4 Avalanche Size Distribution

In the stationary state successive values of minimal wealth w_{min} fluctuates with time. If a certain reference wealth is fixed by hand at $w = w_o$ then the successive w_{min} appear below and above w_o line. One defines a w_o -avalanche as the sequence of successive bipartite trades

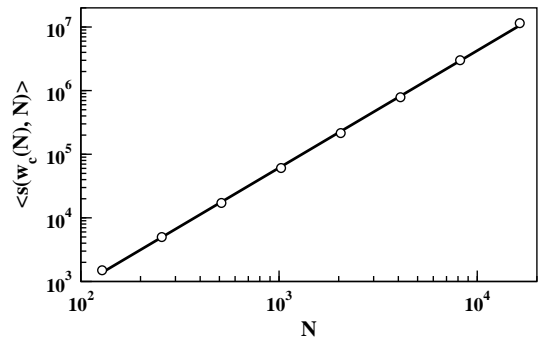


FIG. 11: The average size of the avalanches $\langle s(w_c(N), N) \rangle$ right at the poverty line $w_c(N)$ has been plotted with system size N on a log – log scale. The slope of this curve gives the exponent $\beta = 1.92(2)$.

whose w_{min} values are smaller than w_o . The size s of the avalanche measures the duration of the avalanche i.e., at times t and $t + s + 1$ the $w_{min} > w_o$, whereas at every time step from $t + 1$ to $t + s$ the $w_{min} < w_o$. When w_o is set equal to $w_c(N)$ it is called a critical avalanche. This is explained in Fig. 9 where part of the w_{min} time series for $N = 256$ and $w_c(256) = w_c^{half}(256) = 0.8010$ is displayed discarding the initial $t_{skip} = 5 \times 10^8$ time steps. For $w_o = 0.71$ an avalanche of size 53 breaks into two avalanches of sizes 25 and 27 when w_o is reduced to 0.66. On further reduction of w_o to 0.56 these two avalanche break into even smaller avalanches of sizes 18, 6 and 10, 16 respectively. Thus any avalanche can be splitted into a hierarchy of smaller avalanches if w_o value is lowered [30]. On the other hand if w_o is raised the average avalanche size increases and becomes infinite at certain value of w_o .

At the critical point the distribution of the avalanche life-times has a power law tail in the limit of $N \rightarrow \infty$: $P(s, \infty) \sim s^{-\tau}$. In the stationary state we used $w_o = w_c^{half}(N)$ and measured life-times of a large number of avalanches for different system sizes and plot the probability distributions $P(s, N)$ vs. s using a log – log scale in Fig. 10(a). Each curve has a straight portion in the intermediate regime of the avalanche sizes and this regime becomes gradually larger on increasing N . The direct measurement of slopes in the scaling region gives $\tau(N) = 1.086, 1.091$ and 1.096 for $N = 2^{12}, 2^{13}$ and 2^{14} respectively. A finite-size scaling is very much suitable with the following scaling form:

$$P(s, N)N^{\eta_\tau} \propto \mathcal{F}_\tau(sN^{-\zeta_\tau}) \quad (6)$$

where the scaling function $\mathcal{F}_\tau(x) \sim x^{-\tau}$ in the limit of $x \rightarrow 0$ and $\mathcal{F}_\tau(x)$ approaches zero very fast for $x \gg 1$. The exponents η_τ and ζ_τ fully characterize the scaling of $P(s, N)$ in this case. An immediate way to check the validity of this equation is to attempt a data collapse by plotting $P(s, N)N^{\eta_\tau}$ vs. s/N^{ζ_τ} with trial values of the

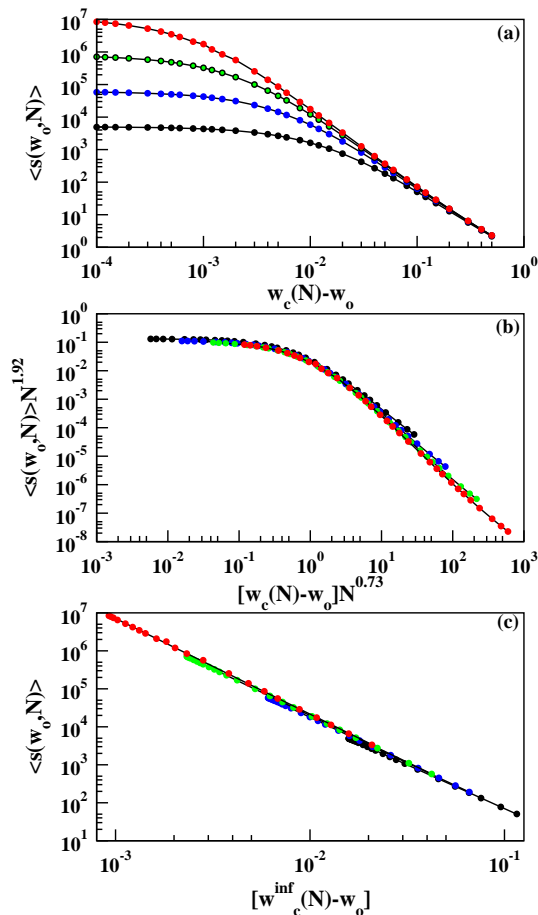


FIG. 12: (Color online) (a) The average value of the avalanche size $\langle s(w_o, N) \rangle$ has been plotted with deviation $w_c(N) - w_o$ from the poverty line $w_c(N)$. The system sizes used are $N = 2^8$ (black), 2^{10} (blue), 2^{12} (green) and 2^{14} (red). The value of γ obtained by extrapolation of slopes is 2.67. (b) Finite size scaling analysis of the data in (a) is shown. The scaling exponents $\eta_\gamma = \beta = 1.92$ and $\zeta_\gamma = 0.73$ gives $\gamma = \eta_\gamma/\zeta_\gamma \approx 2.63$. (c) Plot of the data in (a) but with $w_c(N) = w_c^{inf}(N)$. The slopes for four different system sizes in (a) on extrapolation gives $\gamma = 2.66$. We conclude $\gamma = 2.65(5)$.

scaling exponents. For $1d$ the values for obtaining the best data collapse are found to be $\eta_\tau = 2.44$ and $\zeta_\tau = 2.18$ (Fig. 10(b)). The life-time distribution exponent for $1d$ is therefore $\tau = \eta_\tau/\zeta_\tau \approx 1.12(1)$.

Next we calculated the average value of avalanche life-times $\langle s(w_c, N) \rangle$ right at the critical poverty line. In Fig. 11 we plot this quantity with system size N on a log-log scale. The plot fits excellent to a straight line and its slope gives the value of the exponent $\beta \approx 1.92(2)$ in: $\langle s(w_c, N) \rangle \sim N^\beta$. Assuming the distribution $P(s, N)$ of avalanche sizes holds good up to a cut-off $s_{max} \sim N^{\zeta_\tau}$ one gets a scaling relation $\beta = \zeta_\tau(2 - \tau)$ and our estimates of $\beta = 1.92$, $\zeta_\tau = 2.18$ and $\tau = 1.12$ satisfy this relation very closely.

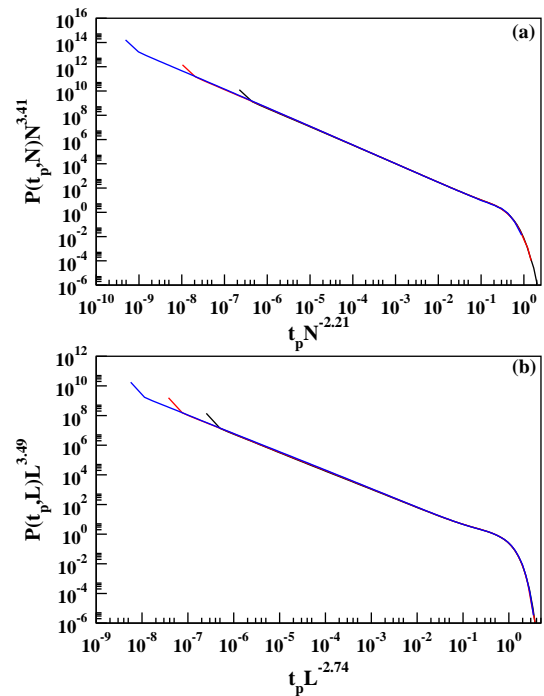


FIG. 13: (Color online) The probability distribution $P(t_p, N)$ of persistence times t_p at the stationary state. (a) The finite-size scaling of the distribution in $1d$ for $N = 2^{10}$ (black), 2^{12} (red) and 2^{14} (blue). From the scaling exponents $\eta_\theta = 3.41$ and $\zeta_\theta = 2.21$ the persistence exponent $\theta = \eta_\theta/\zeta_\theta \approx 1.543$ is obtained. (b) The finite-size scaling of the distribution in $2d$ for $L = 2^8$ (black), 2^9 (red) and 2^{10} (blue). From the scaling exponents $\eta_\theta = 3.49$ and $\zeta_\theta = 2.74$ the persistence exponent $\theta = \eta_\theta/\zeta_\theta \approx 1.274$ is obtained.

The size of the w_o -avalanches are smaller when $w_o < w_c(N)$ and we have studied how the average avalanche size grows as the deviation $(w_c(N) - w_o)$ decreases. Similar to the BS model we assume $\langle s(w_o) \rangle \sim [w_c - w_o]^{-\gamma}$ for $N \rightarrow \infty$. We measured the average size $\langle s(w_o, N) \rangle$ of the w_o -avalanches for different system sizes N and plotted them with $w_c(N) - w_o$ in Fig. 12(a) with $w_c(N) = w_c^{half}(N)$. For all plots on log-log scale the curves are horizontal as deviation $w_c(N) - w_o$ is very small. However as the deviation increases the curves become straight with negative slopes -1.98, -2.15, -2.28 and -2.38 for $N = 2^8, 2^{10}, 2^{12}$ and 2^{14} respectively. These values when extrapolated with $N^{-0.208}$ give $\gamma = 2.67$ for $N \rightarrow \infty$. Again a finite-size scaling has been possible as shown in Fig. 12(b):

$$\langle s(w_o, N) \rangle N^{-\eta_\gamma} \propto \mathcal{F}_\gamma([w_c(N) - w_o] N^{\zeta_\gamma}) \quad (7)$$

where $\mathcal{F}_\gamma(x)$ is another scaling function. From this data collapse the scaling exponents $\eta_\gamma = \beta = 1.92$ and $\zeta_\gamma = 0.73$ with $\gamma = \eta_\gamma/\zeta_\gamma \approx 2.63$ is obtained.

For every system size N there is a value of $w_o = w_c^{inf}(N)$ so that when w_o is raised to this value the

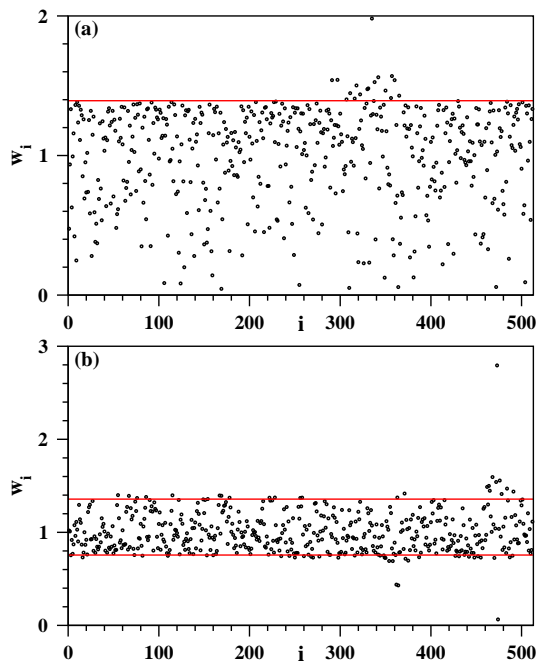


FIG. 14: (Color online) Values of wealth w_i of different agents in the stationary state are plotted with their positions i along a $1d$ lattice for the (a) Maximal Wealth model, the red line is at $w_c^{half}(512) = 1.3924$. (b) mixture of the Minimal Wealth and Maximal Wealth models with probability $p = 1/2$, the red lines correspond to peaks at $w_c(512) = 0.7559$ and at 1.3574 .

avalanche size becomes infinite. This implies that if we plot the data in Fig. 12(a) with respect to $w_c^{inf}(N) - w_o$ then we should be able to see the divergence of average avalanche size instead of saturation of the avalanche sizes. We plot this in Fig. 12(c) using $w_c^{inf}(N) = 0.8167, 0.8169, 0.8170, 0.8172$ for $N = 2^8, 2^{10}, 2^{12}$ and 2^{14} respectively again on a log-log scale. Each curve is a straight line but with different slopes: $-2.31, -2.43, -2.51$ and -2.56 respectively. When these slopes are extrapolated with $N^{-0.31}$ the extrapolated value for $N \rightarrow \infty$ is -2.66 . Our conclusion for the value of the exponent $\gamma = 2.65(5)$.

2.5 Persistence of Wealth in the Stationary State

The time interval between two successive updates of wealth of an agent is known as the persistence time t_p . Different agents have to wait for different amounts of times in general. More specifically agents having small amount of wealth have to wait for very little times. On the other hand potentially rich agents have to wait long enough times. In the stationary state we measure the persistence times for all sites of the lattice and use this data to plot their probability distribution. More precisely we set a clock to each site. Whenever there is a change

of wealth at this site the time is noted and the clock time is reset to zero. At the stationary state we collect a large number of persistence time data and use these data to calculate the persistence time distribution.

We assume a power law variation of the persistence time distribution as $P(t_p) \sim t_p^{-\theta}$ in the limit of $N \rightarrow \infty$. For finite size systems the distributions $P(t_p, N)$ vs. t_p are plotted on a log-log scale (not shown) and the direct measurement of slopes give the $\theta(N)$ values for finite size systems. These values are extrapolated as $N^{-0.494}$ to obtain $\theta = 1.539$ for $N \rightarrow \infty$ in $1d$. In a similar analysis for a $2d$ square lattice of size L using an extrapolation with respect to $L^{-0.565}$ we get $\theta = 1.25$ for $L \rightarrow \infty$.

Persistence exponents are also obtained by the finite-size scaling analysis. In Fig. 13(a) we show the scaling plot of $P(t_p, N)N^{\eta_\theta}$ vs. $t_p N^{-\zeta_\theta}$ with $\eta_\theta = 3.41$ and $\zeta_\theta = 2.21$. This gives $\theta = \eta_\theta/\zeta_\theta = 1.543$ in $1d$. Similar scaling analysis in terms of the system size L in $2d$ square lattice has been performed with $\eta_\theta = 3.49$ and $\zeta_\theta = 2.74$ which gives $\theta = 1.274$ (Fig. 13(b)). Averaging θ values obtained from direct measurement and scaling analysis we conclude $\theta = 1.541(10)$ in $1d$ and $\theta = 1.262(10)$ in $2d$.

3. THE MAXIMAL WEALTH MODEL

Next we studied the Maximal Wealth model where one agent is necessarily the agent with maximal wealth. The other agent being selected randomly with uniform probability from the neighbors of the first agent. Random re-shuffling of wealth takes place in the same way as in the Minimal Wealth model.

In Fig.14(a) we plot again for the Maximal Wealth model the values of wealth w_i of different agents at a certain instant of time in the stationary state with their positions i along an $1d$ lattice of size $N = 512$. In contrast to the similar plot of the Minimal Wealth model in Fig. 1 here an upper cut-off for the wealth has been visible at $w_c^{half}(512) = 1.3924$.

In this case the stationary state wealth distribution $P(w, N)$ takes an opposite shape (Fig. 15(a)). A critical wealth $w_c(N)$ exists here as well. $P(w, N)$ takes a Gaussian form elevated by a constant term $c(N)$ for $w < w_c(N)$, whereas for $w > w_c(N)$ it sharply decreases to zero. The parameters of the Gaussian function (Eqn. (4)) are different for different N and they vary very systematically with N as: $A(N) \approx 30.48 - 133.35N^{-0.361}$, $\mu(N) \approx 3.74 - 6.66N^{-0.85}$ and $\sigma(N) \approx 1.047 + 0.572N^{-0.321}$ and the constant $c(N) \approx 0.031 + 4.265N^{-0.73}$.

The critical value of wealth $w_c(\infty)$ in the asymptotic limit of system sizes has been estimated by the same method as used for the Minimal Wealth model. The $w_c^{half}(N)$ and $w_c^{slope}(N)$ values have been calculated for $N = 2^8, 2^{10}, 2^{12}$ and 2^{14} , extrapolated with $N^{-0.586}$ and $N^{-0.620}$ and the asymptotic values are 1.3610 and 1.3608

	Minimal Wealth model				BS model				Manna model						
	1d		2d		BA graph		N-clique		1d		2d		1d		2d
w_c	0.8175(2)	0.6887(2)	0.6444(2)	0.6076(2)	0.66702(8) [27]	0.328855(4) [30]	0.89199(5) [31]	0.68333(3) [31]							
τ	1.12(1)	1.29(1)	1.50(1)	1.50(1)	1.073(3) [27]	1.245(10) [30]	1.112(6) [32]	1.273(2) [32]							
γ	2.65(5)	1.58(5)	1.02(5)	1.00(5)	2.70(1) [30]	1.70(1) [30]									
π	2.89(5)	3.94(5)	-	-	3.23(2) [30]										
z	2.77(7)														
β	1.92(2)	0.95(2)	0.52(2)	0.50(2)							2			2	
θ	1.541(10)	1.262(10)	1.00(1)	1.00(1)											

TABLE I: Values of different exponents of Minimal Wealth model are compared with those of existing models in the literature.

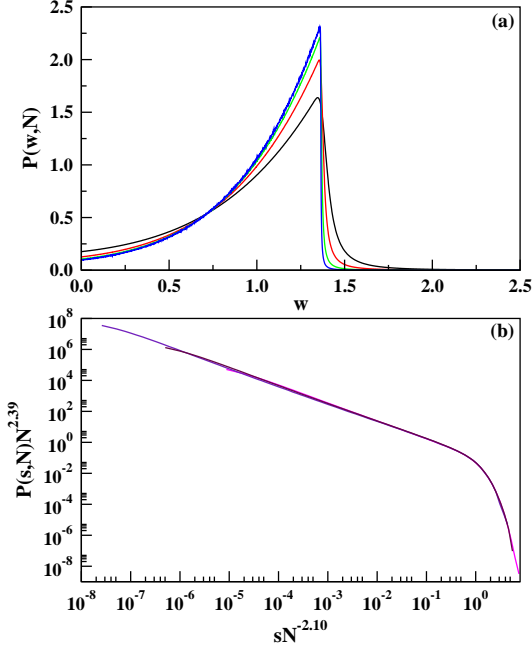


FIG. 15: (Color online) (a) The wealth distribution $P(w, N)$ vs. w for the Maximal Wealth model for $N = 2^8$ (black), 2^{10} (red), 2^{12} (green) and for 2^{14} (blue). (b) Finite-size scaling of the avalanche size distribution $P(s, N)$ at the critical threshold $w_c(N)$ for $N = 2^8$ (black), 2^{10} (red) and 2^{12} (blue). The scaling exponents are $\eta_\tau = 2.39$ and $\zeta_\tau = 2.10$ which gives the exponent $\tau = \eta_\tau/\zeta_\tau \approx 1.14(1)$.

respectively. We conclude $w_c(\infty) = 1.3609(2)$ for $1d$. A similar analysis gives $w_c(\infty) = 1.7076(2)$ for $2d$ square lattice, $1.8895(2)$ for the BA graph and $1.9998(2)$ for the N -clique.

It may appear that the Minimal Wealth and Maximal Wealth models should be symmetric about the average wealth per agent which we have set at $\langle w \rangle = 1$. We have seen above that this indeed not the case since w_c values are 0.8175 and 1.3609 for the Minimal Wealth and Maximal Wealth models respectively. The symmetry between these two models are broken by the presence of a rigid wall at $w = 0$ which means that negative value of wealth of an agent is not allowed.

The avalanche size distributions have been studied as

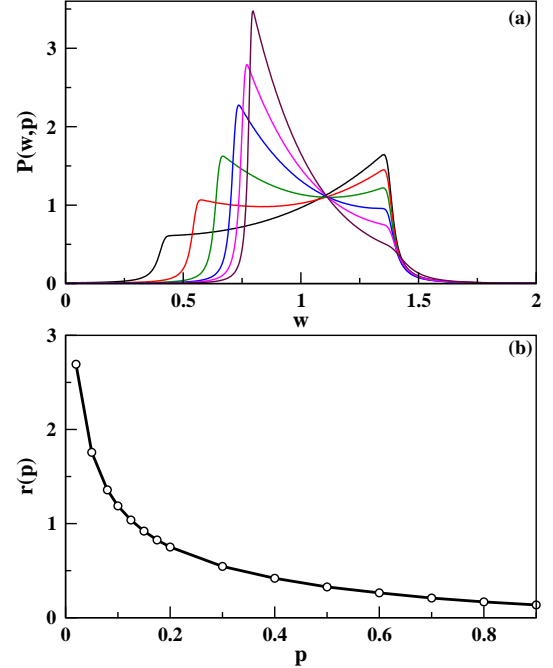


FIG. 16: (Color online) (a) Mixture of Minimal Wealth and Maximal Wealth models with probabilities p and $1 - p$ respectively for $N = 2^9$ and for $p = 0.02$ (black), 0.08 (red), 0.2 (green), 0.4 (blue), 0.6 (magenta) and 0.9 (maroon). (b) Variation of the ratio $r(p)$ of heights of the right peak and the left peak with probability p .

well. A finite-size scaling of these distributions has been done and are plotted in Fig. 15(b) using log – log scale as before for $N = 2^8, 2^{10}$ and 2^{12} . The scaling exponents are $\eta_\tau = 2.39$ and $\zeta_\tau = 2.10$ respectively giving the value of the avalanche size exponent $\tau = \eta_\tau/\zeta_\tau \approx 1.14(1)$.

Finally we have studied a mixture of the Minimal Wealth and Maximal Wealth models. At every bipartite trade the first agent with minimal wealth is selected with probability p or with maximal wealth with probability $1 - p$. The second agent is selected with uniform probability from the neighbors of the first agent. A snapshot of the individual wealth for $p = 1/2$ at the stationary state for different agents has been shown in Fig. 14(b). Here the wealth values are restricted within

a ‘wealth-band’ with sharp cut-offs at a high and a low end. Consequently the shape of the wealth distribution $P(w, p)$ has double peaks for all N and we plot the distribution in Fig. 16(a) for $N = 2^9$. Portion of the distribution between the peaks fits excellent to elevated Gaussian distributions with different parameter values for different values of p in the range between 1/2 and 1. On the two sides of this region the distribution decays to zero very fast. The figure shows the plot of $P(w, p)$ vs. w for $p = 0.02, 0.08, 0.2, 0.4, 0.6$ and 0.9 . In Fig. 16(b) we plot the ratio $r(p)$ of the heights of right peak and the left peak with the probability p .

4. CONCLUSION

Social inequality in terms of economic strengths is ubiquitous for the people of all countries. Perhaps this inequality acts as the major driving force behind the advancement of society. Consequently the mechanism that establishes this inequality in a society is an important issue and attracted the attention of researchers over the last century. Here we have studied a modified version of the conservative self-organized extremal model introduced by Pianegonda et. al. which is motivated by the wealth distribution in a society. In this model the entire wealth of the society is strictly conserved. It evolves by a trade dynamics that takes the society from equality (or any other initial wealth distribution) to a stationary state where strong social inequality is present. The dynamics is an infinite sequence of stochastic bipartite tradings where one of the agents has the globally minimal value of wealth, the other one being selected randomly from the neighbors of the first agent. Our numerical study reveals that this model is one of the simplest models of Self-organized Criticality where the stationary state is non-ergodic. This model is very similar to the self-organized critical Bak-Sneppen model for the ecological evolution of interacting species. Using numerical simulation we have estimated a number of critical exponents for this model on an $1d$ regular lattice, $2d$ square lattice, the Barabási - Albert scale-free graph and on the N -clique graph. We present evidences which suggest that this model does not belong to the universality class of either the Bak-Sneppen model or the Manna model of Self-organized Criticality. This model belongs to a new universality class perhaps because of strict conservation of wealth is maintained in its dynamical rules.

G. Mukherjee thankfully acknowledges the associate-ship in S. N. Bose National Centre for Basic Sciences, Kolkata under the Extended Visitor and Linkage programme. Comments from B. K. Chakrabarti, A. Chatterjee, D. Dhar, J. R. Iglesias, J. Kertesz, P. K. Mohanty

and P. Pradhan are thankfully acknowledged.
manna@bose.res.in

-
- [1] V. Pareto, *Cours d'economie Politique* (F. Rouge, Lausanne, 1897).
 - [2] en.wikipedia.org/wiki/Pareto_distribution.
 - [3] W. Souma, *FRACTALS*, **9**, 463 (2001).
 - [4] A. A. Drăgulescu, V. M. Yakovenko, *Eur. Phys. J. B* **299**, 213 (2001).
 - [5] J. R. Iglesias, *Science and Culture*, **76**, 437 (2010).
 - [6] A. A. Drăgulescu, V. M. Yakovenko, *Eur. Phys. J. B* **17**, 723 (2000).
 - [7] V. M. Yakovenko and J. B. Rosser, *Rev. Mod. Phys.* **81**, 1703 (2009).
 - [8] J. Angle, *Social Forces* **65**, 293 (1986).
 - [9] A. Chakraborti, B. K. Chakrabarti, *Eur. Phys. Jour. B*, **17** 167 (2000).
 - [10] K. Bhattacharya, G. Mukherjee and S. S. Manna, in *Econophysics of Wealth Distributions*, (Springer Verlag, Milan, 2005).
 - [11] M. Patriarca, A. Chakraborti, K. Kaski, *Phys. Rev. E* **70**, 016104 (2004).
 - [12] A. Chatterjee, B. K. Chakrabarti, S. S. Manna, *Physica A* **335** 155 (2004), A. Chatterjee, B. K. Chakrabarti, S. S. Manna, *Physica Scripta T* **106** 36 (2003).
 - [13] P. K. Mohanty, *Phys. Rev. E*, **74**, 011117 (2006).
 - [14] U. Basu and P. K. Mohanty, *Eur. Phys. J. B* **65**, 585 (2008).
 - [15] A. Chakraborty and S. S. Manna, *Phys. Rev. E* **81**, 016111 (2010).
 - [16] A. Chatterjee and B. K. Chakrabarti, *Euro. Phys. Journal B* **60**, 135 (2007).
 - [17] S. Pianegonda, J. R. Iglesias, G. Abramson, J. L. Vega, *Physica A*, **322**, 667 (2003).
 - [18] J. R. Iglesias, S. Concalves, S. Pianegonda, J. L. Vega and G. Abramson, *Physica A*, **327**, 12 (2003).
 - [19] P. Bak and K. Sneppen, *Phys. Rev. Lett.* **71**, 4083 (1993).
 - [20] P. Bak, C. Tang and K. Wiesenfeld, *Phys. Rev. Lett.* **59**, 381 (1987).
 - [21] P. Bak, *How Nature Works: The Science of Self-Organized Criticality*, (Copernicus, New York, 1996).
 - [22] S.S. Manna, *J. Phys. A* **24**, L363 (1991).
 - [23] M. Basu, U. Gayen and P. K. Mohanty, arXiv:1102.1631.
 - [24] A. Ghosh, U. Basu, A. Chakraborti and B. K. Chakrabarti, *Phys. Rev. E*, **83**, 061130 (2011).
 - [25] S. Lübeck, *Int. Jour. Mod. Phys. B* **18**, 3977 (2004).
 - [26] A.-L. Barabási and R. Albert, *Science*, **286**, 509 (1999).
 - [27] P. Grassberger, *Phys. Lett. A* **200**, 277 (1995).
 - [28] S. S. Manna, *Phys. Rev. E.*, **80**, 021132 (2009).
 - [29] B. B. Mandelbrot, *The Fractal Geometry of Nature*, (1982) W.H. Freeman, ISBN 0-7167-186-9.
 - [30] M. Paczuski, S. Maslov and P. Bak, *Phys. Rev. E* **53**, 414 (1996).
 - [31] S. Lübeck and P. C. Heger, *Phys. Rev. Lett.* **90**, 230601 (2003).
 - [32] H. N. Huynh, G. Pruessner and L. Y. Chew, *J. Stat. Mech.* 09024 (2011).